Hydrogeology Journal (2024) 32:2051–2065
https://doi.org/10.1007/s10040-024-02846-3

PAPER

Evaluation of groundwater travel time through a multilayered aquifer using multiple tracers and a novel transport approximation

Meredith B. Martinez[1] · **Mark A. Widdowson**[1]

Received: 28 February 2024 / Accepted: 14 October 2024 / Published online: 15 November 2024

Abstract

Aquifer long-term replenishment (ALTR) is a managed aquifer recharge (MAR) strategy by which reclaimed water is continuously delivered by injection wells to depleted, confined aquifer systems to increase groundwater storage and increase the potentiometric surface over space and time. One implication of large-scale continuous recharge is a large radial impact and the need to quantify transport in radially extensive strata. The use of an artificial tracer can be cost-prohibitive as the radial front moves further from the injection well. This investigation employs a novel approximation for radial transport to track the radial front of recharge, injectate constituents and simulation of tracer breakthrough concentrations under transient recharge rates, variable depth-dependent flow distributions over time, and variable influent concentrations. Six constituents—sulfate, chloride, total organic carbon (TOC), fluoride, 1,4-dioxane and N-nitrosodimethylamine (NDMA)—were chosen to evaluate conservative transport and semiqualitatively assess attenuation of nonconservative constituents relative to conservative tracers. Results indicate that sulfate acted as the most effective conservative tracer for characterization of transport and travel times at the study site. The analytical model was modified to account for variable operations at the MAR demonstration facility and was effective in simulating breakthrough curves over the period of performance, particularly sulfate concentrations at a monitoring well located 104 m from the injection well. The behavior of the remaining constituents is discussed, and the qualities of an effective intrinsic tracer for future ALTR projects are identified.

Keywords Managed aquifer recharge (MAR) · Injection wells · Tracer tests · Analytical solutions/modelling · Virginia Coastal Plain

Introduction

Managed aquifer recharge (MAR) encompasses a range of water reuse strategies including aquifer storage and recovery (ASR), aquifer storage transfer and recovery (ASTR), and artificial recharge (AR) projects (Pyne 2006; Ringleb et al. 2016; Dillon et al. 2019). Recently, AR has expanded beyond short-term replenishment goals to larger-scale projects designed to increase aquifer storage capacity and improve water security. Aquifer long-term replenishment (ALTR) involves continuous delivery of treated water to confined aquifer systems using multiple recharge wells to increase groundwater storage and raise the regional potentiometric surface (Martinez et al. 2022). As the ALTR concept is designed for the delivery of continuous recharge at relatively large pumping volumes over time, verifying the potential impacts on groundwater quality may require tracking the front of recharge waters over relatively long distances. Injection wells are a practical necessity to recharge confined aquifer systems with designs ranging from single-screen wells to multiscreen wells, depending on site-specific hydrostratigraphy. Monitoring chemical transport of recharge waters into and within aquifer systems at MAR projects employing multiscreen injection wells is particularly challenging without methods to quantify the flow distribution and monitoring infrastructure and models to track the radial front of recharge.

The forced gradient tracer test (FGTT) is a field method applicable to ALTR or other injection well-based MAR systems for characterizing radial advective–dispersive solute transport and to quantify flow distribution and aquifer

✉ Mark A. Widdowson
mwiddows@vt.edu

[1] The Charles E. Via Jr. Department of Civil and Environmental Engineering, Virginia Tech, 750 Drillfield Drive, 200 Patton Hall, Blacksburg, VA 24061, USA

properties in stratified aquifers (Molz et al. 1988). Single well, continuous injection tracer tests performed in a stratified confined aquifer were monitored using multilevel samplers in a nearby observation well to model advective–dispersive transport and quantify vertical variation in hydraulic conductivity (Güven et al. 1985; Molz et al. 1985). Molz et al. (1986) conducted a two-well tracer test in the same confined aquifer using injection and recovery wells operating at similar flow rates, confirming the validity of FGGT implementation over a larger scale. MAR systems involving continuous recharge delivered using injection wells can mimic a single-well FGGT where injectate is delivered at one well and tracer breakthrough is observed at monitoring wells.

Davis et al. (1985) outlined and discussed commonly used artificial and intrinsic tracers, including temperature, ions, dyes, dissolved gases, stable isotopes, and radionuclides. Multitracer tests have also been used to characterize aquifer properties as well as flow between aquifer systems (e.g., Reimus et al. 2003; Goderniaux et al. 2010; Hillebrand et al. 2015; Hadi et al. 2016; Suckow et al. 2020). Sanford et al. (2017) found that incorporating multiple tracer concentrations into an advective-transport model was useful to identify the existence of a dual-porosity system and constrain transport parameters. Gerenday et al. (2020) showed that the use of multiple tracers (sulfur hexafluoride and potassium bromide) was effective to assess hydrologic conditions such as porous media saturation in unconfined aquifers at MAR sites where the primary method of recharge was infiltration basins supported by injection wells.

For application to ALTR and other MAR projects, artificial tracers such as bromide or carbamazepine added to recharge water may be effective in determining aquifer characteristics. However, the composition of the recharge injectate itself can be leveraged as an initial and potentially long-term valuable tracer tool—for example, studies suggest that the water used for recharge in an ASR project is sufficient to be used for a large-scale tracer test (Williams 2000; Pavelic et al. 2006). Chloride or other intrinsic characteristics of recharge water, such as specific conductance, have been employed as tracers on ASR projects (Mirecki et al. 1998; Pavelic et al. 2006). Provided that the recharge characteristics are significantly different from native groundwater characteristics, using recharge injectate eliminates the potential high cost associated with injecting large amounts of artificial tracer to characterize a whole site, since the recharge itself becomes an intrinsic tracer.

One promising avenue of research is the analysis of multiple indicators within injectate for large-scale site characterization. In recharge wells where native groundwater characteristics vary by screen depth, identifying multiple intrinsic tracers to quantify breakthrough at all screens is important to understand transport fully. Furthermore, the use of an intrinsic tracer to quantify flow and transport in multiple strata through a single multiscreen recharge well is novel, since most studies of multilayer or multiaquifer systems implement either multiple injection wells (Young and Benton 1990; Hadi et al. 2016), borehole dilution (West and Odling 2007), or pumping test drawdown analysis (Hunt 1986; Székely 1992; Wu et al. 2015) to characterize the aquifer system.

For the analysis of concentration breakthrough data, solutions for constituent transport have been developed to describe advective–dispersive axisymmetric transport in the case of pumping or recharge conditions (Chen 1985; Hsieh 1986; Moench 1989, 1995; Goltz and Oxley 1991; Novakowski 1992; Lai et al. 2016). The majority of existing axisymmetric analytical models assume constant operating conditions (i.e., the velocity field is not treated as a function of time) and constant influent concentrations. Chen et al. (2012) considered radial solute transport under variable flow and concentration conditions and provided a semianalytical solution to evaluate the relative concentration by transforming the time domain to the cumulative flow domain within a single-screen recharge or pumping well. Accounting for the flow distribution of recharge through multiple well screens would be computationally intensive in situations where dynamic flow distributions are observed. However, this is a key requirement given that ALTR and other MAR projects operate at transient recharge rates and the concentration of intrinsic tracers typical vary with time on a regular basis; furthermore, existing analytical solutions are limited to single-screen wells.

This study examines the transport of multiple intrinsic tracers through a multiscreen recharge well at an ALTR demonstration project. The FGGT concept is applied to analyze tracer transport over a distance of 104 m and a timespan of 3.5 years. Starting with the initiation of recharge in May 2018, operational conditions varied over time as a result of several extended periods for maintenance, regular short-term pumping periods to maintain recharge well injectivity, and one extended pumping event. The objective of this study was to use multiple intrinsic tracer concentration data to characterize solute transport due to the delivery of injectate to a complex multistrata aquifer system and to evaluate travel time within each strata using a novel approximation for quantifying tracer breakthrough under transient flow, dynamic flow distribution, and variable influent concentration conditions. Furthermore, the study aims to describe attenuation of nonconservative constituents relative to a conservative tracer (e.g., sorption, biodegradation, mobile/immobile mass transfer), identify qualifying characteristics for effective tracers, and evaluate the reliability of the novel approximation. This study is unique in that it allows for comparison to a large-scale field experiment to aid in model validation.

Methods

Project description and hydrogeology

In 2018 Hampton Roads Sanitation District (HRSD) initiated an AR experiment at the Sustainable Water Initiative for Tomorrow (SWIFT) Research Center (SRC) in Suffolk, Virginia, United States of America. Martinez et al. (2022) described the project background and location in detail including lessons learned from the initial demonstration phase at the SRC. The SWIFT project is a large-scale MAR project based on the ALTR concept designed to treat effluent from HRSD water reclamation facilities to drinking water standards and then recharge the Potomac Aquifer System (PAS) through injection wells located on site.

The PAS is the largest and deepest aquifer system in the Virginia Coastal Plain and serves as the primary source of groundwater withdrawals in eastern Virginia, accounting for ~74% of the region's groundwater withdrawals (Heywood and Pope 2009). The PAS in Virginia ranges in thickness from 0 m at its western margin to more than 2000 m along the Atlantic coast (McFarland 2013). Prior to development, groundwater flowed through the PAS generally eastward from recharge areas along its western margin to estuarial and marine discharge areas in the east (Heywood and Pope 2009). With insufficient natural recharge to counterbalance groundwater withdrawals of 380 ML/day from numerous pumping centers in the PAS, potentiometric surface declines as great as 60 m have been observed over the past 60–70 years (McFarland 2013).

The PAS is comprised of primarily fluvial-deltaic coarse-grained sands and gravels with interbedded clays of varying thicknesses deposited by a fluvial depositional complex spanning the Virginia Coastal Plain ~100–145 Ma (McFarland and Bruce 2006). Due to the nature of the interbedded clays, confining units within the PAS function as local barriers but are not homogeneous and are often discontinuous across the extent of the PAS (McFarland and Bruce 2006; Heywood and Pope 2009). The US Geological Survey (USGS) originally subdivided the PAS into upper, middle, and lower Potomac Aquifers (UPA, MPA, and LPA, respectively) separated by intervening confining units (Meng and Harsh 1988). However, since 2013, the USGS has considered the PAS regionally as a single aquifer. Nevertheless, for the purpose of this study and based on the specific site hydrostratigraphy and solute transport behaviour, the PAS is treated as three distinct hydrostratigraphic units and analyzed separately. The PAS at the SRC is present beginning with the UPA at 150 m below ground surface (bgs) and extending to bedrock at a depth of 600 m bgs.

Site description

Figure 1 depicts the primary SRC test infrastructure, which consists of one 11-screen recharge well (TW-1), one depth-discrete monitoring well (MW-SAT), and three conventional monitoring wells screened in the upper, middle, and lower strata of the PAS (MW-UPA, MW-MPA, and MW-LPA, respectively). TW-1 has 11 discrete screens located in the UPA, MPA, and LPA (Table 1), while MW-SAT is located 15.2 m from TW-1 and is screened at identical depths. The three multiscreen monitoring wells (MW-UPA, MW-MPA, and MW-LPA) are located 104, 119, and 134 m from TW-1, respectively. The conventional wells were screened at depth based on geophysical logging during drilling, reflecting the most transmissive depths of the PAS (Table 2), while not exactly matching screen depths at TW-1.

Due to the relatively long travel times in the MPA and LPA in comparison to travel time from TW-1 to MW-UPA, this study primarily focuses on transport in the UPA only, although the discussion and conclusions will be extrapolated to the MPA and LPA. Tracer concentration data collected at the MW-MPA is presented to demonstrate the potential limitations of this approach. A simplified figure of screen depths and hydrostratigraphy in the UPA is included in Fig. S1 of the electronic supplementary material (ESM).

Operating conditions at the recharge well (concentrations and recharge rate) were incorporated as boundary conditions and input to the radial transport model, respectively, for analysis of tracer breakthrough. Recharge operations at the SRC during the period of performance were separated into nine phases with recharge and pumping volume for each phase listed in Table 3. Because of the depth of the PAS (Table 2) and multiple overlying confining units, any impact of recharge due to precipitation is considered negligible. The total duration and a detailed description of each operating condition per phase are provided in Tables S1 and S2 of the ESM, respectively.

Tracer selection

Breakthrough at MW-SAT was identified using constituents of SWIFT water as an intrinsic tracer (Bullard et al. 2019). The term SWIFT water is used for the SRC effluent that served as the source of recharge at TW-1. Specific conductivity was used as a surrogate of chloride in SWIFT water due to the ability to measure at a high temporal resolution and the availability of a cost-effective handheld conductivity probe. While specific conductivity served as an acceptable indicator at MW-SAT, the use of multiple tracers was suggested for MW-UPA due to the high variation in native groundwater characteristics between screens 1–4. Specific conductivity at MW-UPA was not significantly different than SWIFT water specific conductivity (1247 ± 184 μS/cm).

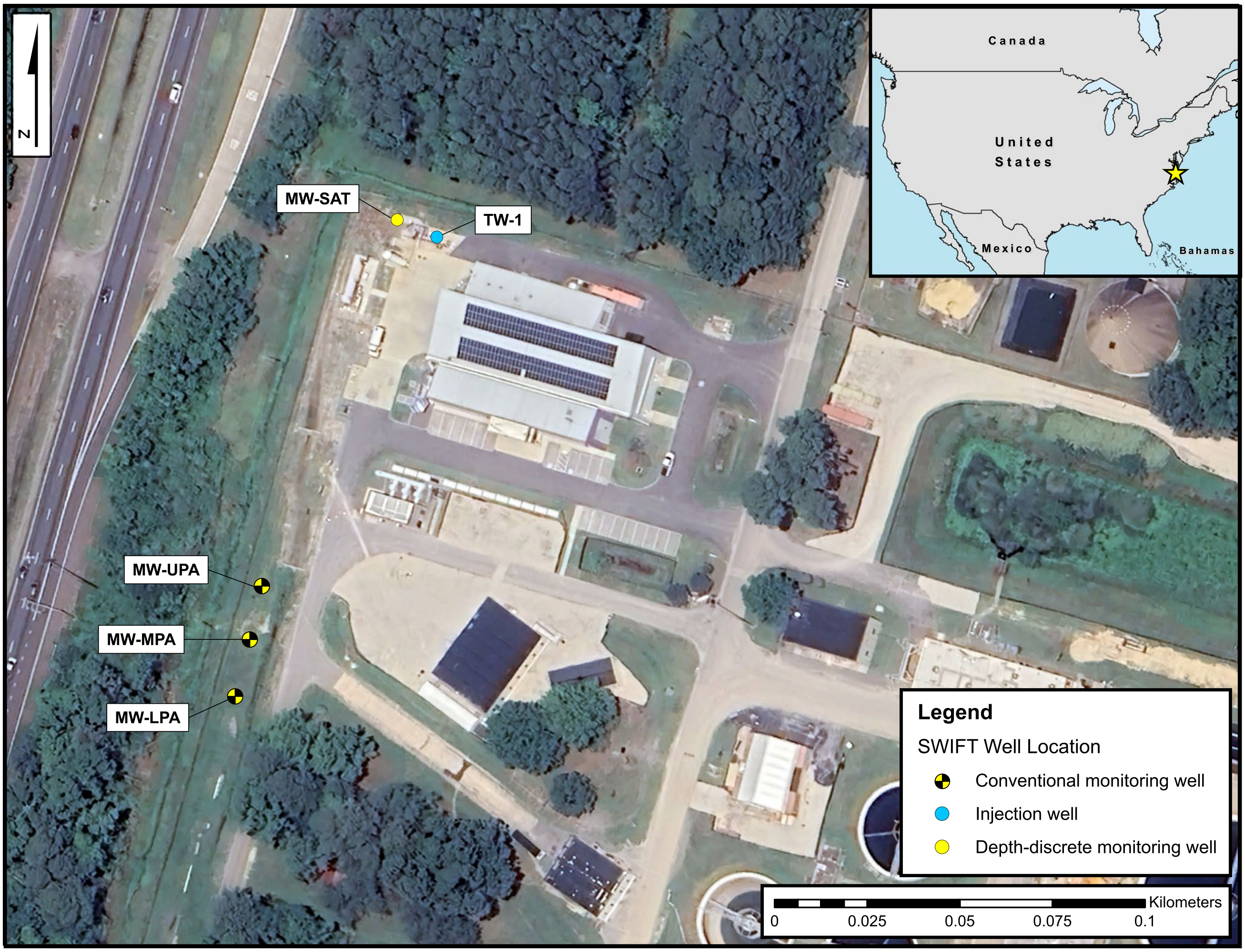

Fig. 1 Site map of the SWIFT Research Center. TW-1 is the injection well, MW-SAT is the depth discrete sampling system, and MW-UPA, MW-MPA, and MW-LPA are the Upper, Middle, and Lower Potomac conventional monitoring wells, respectively

Although conductivity may not be an acceptable indicator at MW-UPA, it will likely indicate a preliminary breakthrough at monitoring wells MW-MPA and MW-LPA.

Consequently, a review of the sampled constituents was undertaken to identify other constituents in SWIFT water that could be analyzed as conservative or semiconservative tracers. Of 88 potential constituents monitored by the Central Environmental Lab (CEL) at HRSD, candidates were narrowed by sample frequency, detection of the constituent above the detection limit in either SWIFT water or the conventional well, and the nature of the constituent. Chloride, fluoride, sulfate, 1,4-dioxane, N-nitrosodimethylamine (NDMA), and total organic carbon (TOC) were identified as potential constituents of interest. Chloride, fluoride, and sulfate were chosen because of their potential to serve as conservative tracers. Previous work on soil columns at this site indicated that a measurable fraction of TOC present in SWIFT water degrades during transport and 1,4-dioxane and NDMA may degrade during transport (Dziura 2020), providing an opportunity to compare a conservative transport model to observations at MW-UPA and semiquantitatively assess the nature of the constituents within the aquifer system.

Background groundwater concentrations for the chosen constituents at MW-SAT (screens 1–11) and the conventional wells are listed in Table 4. The elevated TOC concentration at MW-SAT relative to the conventional monitoring wells was attributed to differences in the construction of the wells. Site geochemistry featured a neutral pH (7.1–7.2) in all units of the PAS, brackish concentrations of TDS (3800–5200 mg/L), and sodium chloride groundwater facies. Groundwater exhibited dissolved oxygen (DO) concentrations (<0.5 mg/L) and oxidation–reduction potential indicative of anoxic conditions in each PAS unit with iron reduction as the predominating redox process.

Table 1 Well screen depth and length of screen in wells TW-1 and MW-SAT. *mbgs* meters below ground surface

Aquifer zone	Starting depth (mbgs)	Ending depth (mbgs)	Screen length (m)
Upper Potomac Aquifer (UPA)			
Screen 1	153.9	161.5	7.6
Screen 2	167.6	181.4	13.7
Screen 3	202.7	207.3	4.6
Screen 4	219.5	230.1	10.7
Middle Potomac Aquifer (MPA)			
Screen 5	249.9	254.5	4.6
Screen 6	262.1	271.3	9.1
Screen 7	275.8	280.4	4.6
Screen 8	294.1	301.8	7.6
Screen 9	320.0	332.2	12.2
Lower Potomac Aquifer (LPA)			
Screen 10	374.9	406.9	32.0
Screen 11	417.6	426.7	9.1

Table 2 Well screen depth and length of screen in the conventional monitoring wells. *mbgs* meters below ground surface

Aquifer zone	Starting depth (mbgs)	Ending depth (mbgs)	Screen length (m)
MW-UPA (distance from TW-1 = 103.6 m)			
Screen 1	157.0	172.2	15.2
Screen 2	178.3	184.4	6.1
Screen 3	201.1	205.7	4.6
Screen 4	216.4	225.5	9.1
MW-MPA (distance from TW-1 = 118.9 m)			
Screen 1	262.1	280.4	18.3
Screen 2	297.2	301.8	4.6
Screen 3	313.9	332.2	18.3
MW-LPA (distance from TW-1 = 134.1 m)			
Screen 1	384.0	402.3	18.3
Screen 2	411.5	429.8	18.3

Tracer monitoring

Fluoride, sulfate, and chloride samples were collected and analyzed for SWIFT water and at MW-UPA using EPA Method 300.0 (Pfaff 1993). SWIFT water samples for these three constituents were collected approximately once per day when the SRC was recharging water to the PAS. As fluoride was the originally selected constituent to monitor breakthrough based on its behavior at MW-SAT, samples for fluoride analysis were taken at MW-UPA daily. Sulfate and chloride samples were taken approximately once per week, although frequency did vary over time and with recharge status at TW-1. Due to their cost-effectiveness of sampling, fluoride, sulfate, and chloride were the most frequently sampled constituents. 1,4-dioxane samples were collected and analyzed using EPA Method 522 (Munch and Grimmett 2008), while NDMA samples were collected and analyzed using EPA Method 521 (Munch 2005) and quality control (QC) samples were used to evaluate the quality of data according to each analyzation method. TOC data were collected and analyzed using standard methods 5310B (Lipps et al. 2023). The exact number of samples for each data set included in the breakthrough model is included in Table 5.

Figure 2 depicts the temporal variability of the six constituents in SWIFT water and Table 6 summarizes the variability of influent concentrations in SWIFT water of the six tracer constituents examined during the study duration. Sulfate was consistently measured in SWIFT water and was significantly different (>3 standard deviation, SD) from background concentrations of sulfate in MW-UPA. TOC had the most predictably variable influent concentration due to the use of granular activated carbon (GAC) during advanced treatment. Fresh GAC had high rates of TOC removal during the treatment process, but as the carbon was exhausted, TOC concentrations increased over time. During the 2018–2019 well rehabilitation process, which also included a treatment process shutdown, the carbon in the two GAC contactors was replaced, and TOC concentrations dropped and increased again as treatment restarted. Once TOC concentrations reached 4 mg/L, flow was split between two carbon contactors to maintain a TOC concentration between 3.5 and 4.0 mg/L.

The average chloride concentration used for the injection well concentration in model 2 was 202.86 mg/L. Influent chloride data showed an initial period (days 0–110) with an average concentration of 226 mg/L followed by a second period (days 110–203) with average influent chloride concentration measuring 168.5 mg/L. Chloride concentrations after the well rehabilitation was an average of 206.6 mg/L with an SD of 55.3 mg/L. Fluoride was measured daily at the SRC and concentrations were consistent and nonvariable. Concentrations were significantly different from fluoride concentrations in MW-SAT screens 1–4 and MW-UPA. 1,4-dioxane and NDMA were measured at lower frequencies than the previous four constituents due to the cost of analysis.

Radial transport model development

Bullard et al. (2019) previously demonstrated the application of a radial transport model to simulate tracer breakthrough at MW-SAT under transient flow conditions during the initial operations of recharge at TW-1, which included short-term stoppages and pumping events. As longer-term operations at the SRC were transient and included intermittent periods of recharge, backflush (pumping), and

Table 3 Recharge and pumping volume during the observation period. All volumes are given in thousand cubic meters (10^3 m^3). Parentheses indicate negative flow (i.e., pumping volume)

Phase	Start time (mm/dd/yy hh:mm)	End time (mm/dd/yy hh:mm)	Length (days)	Total recharge volume	Total pumping volume	Net recharge volume
1	05/15/18 14:15	08/02/18 17:00	79.11	156.001	–4.463	151.534
2	08/02/18 17:00	08/21/18 14:45	18.91		–100.105	–100.105
3	08/21/18 14:45	11/21/18 01:15	91.44	222.628	–3.941	218.687
4	11/21/18 01:15	04/26/19 08:00	156.28	0.409	–2.862	–2.453
5	04/26/19 08:00	04/29/19 07:00	2.96	0.019	–17.080	–17.057
6	04/29/19 07:00	12/25/20 17:15	606.43	1235.414	–127.625	1107.785
7	12/25/20 17:15	04/09/21 13:15	104.83	2.199		2.199
8	04/09/21 13:15	04/14/21 12:00	4.95	0.575	–24.969	–24.393
9	04/14/21 12:00	11/02/21 02:15	201.59	383.519	–53.423	330.092

Table 4 Pre-recharge native groundwater concentrations of identified constituents of interest. Individual screens in MW-SAT are noted with S-[screen number] (e.g., MW-SAT S-1 for screen 1). 1,4-dioxane and NDMA are not included because both were below detection limits (0.06 µg/L and 2 ng/L, respectively) in every screen in MW-SAT and the conventional wells. For the detected constituents, 1 standard deviation (SD) is listed in parentheses. Measured TOC in MW-SAT is likely higher than actual native groundwater concentrations due to interference during installation

Location	Constituent				
	Conductivity (µS/cm)	Chloride (mg/L)	Fluoride (mg/L)	Sulfate (mg/L)	TOC (mg/L)
MW-SAT S-1	1463 (±6)	162 (±5)	4.40 (±0.2)	23 (±1)	1.09 (±0.03)
MW-SAT S-2	3696 (±137)	1450 (±161)	2.76 (±0.2)	89 (±15)	1.08 (±0.16)
MW-SAT S-3	7690 (±101)	2030 (±89)	1.74 (±0.1)	122 (±11)	1.05 (±0.21)
MW-SAT S-4	7790 (±106)	1900 (±446)	1.52 (±0.2)	129 (±10)	1.05 (±0.13)
MW-SAT S-5	9873 (±94)	3716 (±90)	ND[a]	235 (±13)	0.99 (±0.33)
MW-SAT S-6	12548 (±73)	3227 (±993)	ND[a]	203 (±13)	1.16 (±0.38)
MW-SAT S-7	12088 (±148)	3593 (±39)	ND[a]	154 (±23)	4.88 (±0.38)
MW-SAT S-8	5806 (±190)	2070 (±131)	ND[a]	149 (±29)	1.63 (±0.26)
MW-SAT S-9	5768 (±44)	1947 (±154)	ND[a]	93 (±12)	2.30 (±0.11)
MW-SAT S-10	13551 (±44)	3800 (±649)	ND[a]	248 (±14)	2.76 (±1.03)
MW-SAT S-11	16763 (±104)	5290 (±155)	0.43 (±0.1)	279 (±45)	5.02 (±1.05)
MW-UPA	1133 (±223)	117 (±2)	4.07 (±0.04)	23 (±0.3)	0.31 (±0.04)
MW-MPA	4743 (±210)	1133 (±31)	0.67 (±0.03)	92 (±4)	ND[b]
MW-LPA	13623 (±1669)	4313 (±255)	ND[a]	226 (±13)	0.20 (±0.01)

[a]Detection limit = 0.50 mg/L
[b]Detection limit = 0.20 mg/L

Table 5 Number of SWIFT water influent and MW-UPA samples included in the breakthrough model

Constituent	SWIFT water influent	MW-UPA
Sulfate	455	264
TOC	357	128
Chloride	456	147
Fluoride	594	874
1,4-dioxane	97	71
NDMA	101	71

shutdown (no flow at the well) combined with variations in recharge concentrations, the Bullard et al. (2019) model was updated to simulate SRC operations.

Equation (1) describes tracer concentrations, $C_i(r,t)$ during radial flow at each screened interval (modified from Charbeneau 2000):

$$C_{s,i}(r,t) = C_{\mathrm{B},s} + \frac{(C_{\mathrm{F}} - C_{\mathrm{B},s})}{2} * \operatorname{erfc}\left[\frac{r - R^*_{s,i}}{\sqrt{\frac{4}{3}\alpha_{\mathrm{L},s} R^*_{s,i}}}\right] \tag{1}$$

where $C_{\mathrm{B},s}$ is the background concentration within the screen of interest, C_{F} is the influent concentration, r is the radial distance from the injection well, t is the time since the start of injection, $\alpha_{\mathrm{L},s}$ is the screen-specific longitudinal dispersivity, $R^*_{s,i}$ is the mean displacement of the front, n is the screen-specific effective porosity, and b is the screen length of interest.

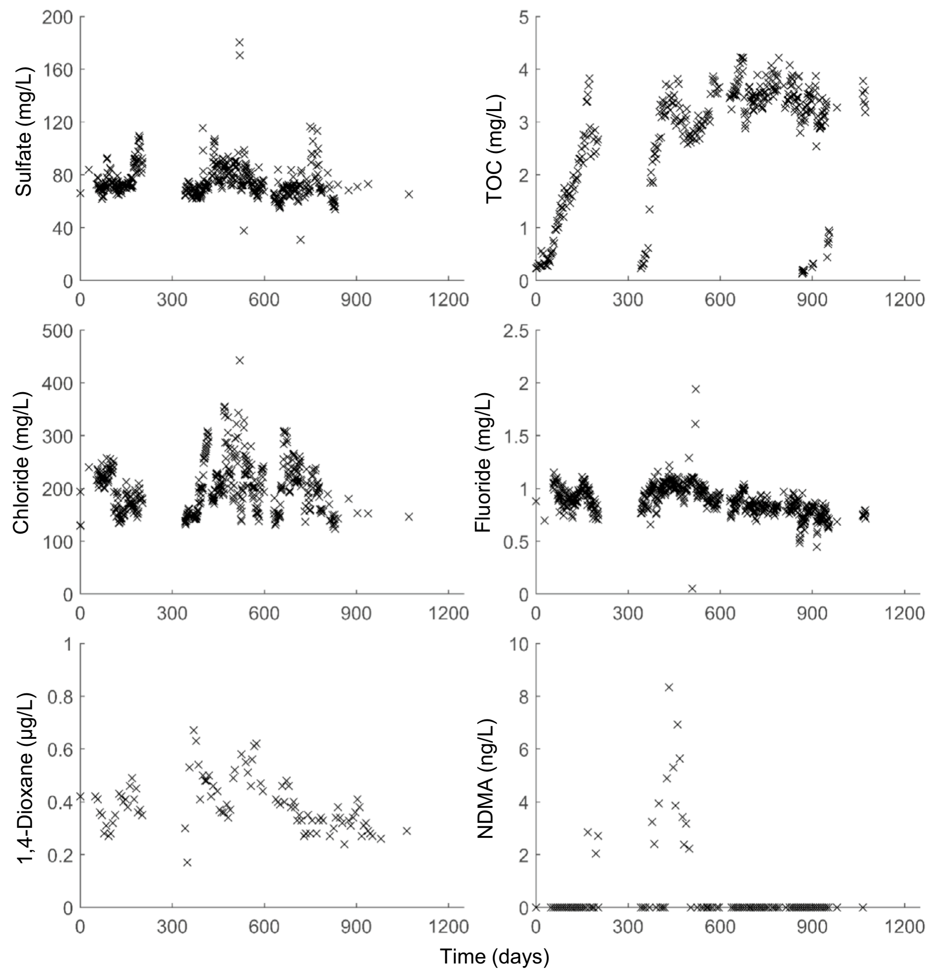

Fig. 2 SWIFT water concentrations of constituents of interest at TW-1. These concentrations were used as influent concentration values for the variable-concentration model

Table 6 SWIFT water characteristics for tracer constituents. Concentration values are noted in mg/L unless otherwise indicated via footnote. *SD* standard deviation

Constituent	No. of measurements	No. of detections	Average value	SD	Min value	Max value
Sulfate	455	455	75.23	12.89	30.80	180.30
TOC	357	357	2.73	1.12	0.13	4.23
Chloride	456	456	202.86	50.38	123.64	545.47
Fluoride	594	594	0.89	0.14	0.05	1.94
1,4-dioxane[a]	97	97	0.39	0.10	0.17	0.67
NDMA[b]	101	16	3.96	1.76	0.00[c]	8.34

[a]Concentration values are measured in µg/L

[b]Concentration values are measured in ng/L

[c]Indicates nondetected

To account for changing influent concentrations, Eq. (1) was modified to incorporate changes in each measured influent concentration with time:

$$t_i < t_j \qquad \begin{aligned} C_{s,i,j}(r,t) &= 0 \\ R^*_{s,i}(t) &= 0 \\ V^*_{s,i}(t) &= 0 \end{aligned} \tag{2}$$

$$t_i \geq t_j \qquad C_{s,i,j}(r,t) = \frac{\Delta C_{\mathrm{F}}}{2} * \mathrm{erfc}\left[\frac{r - R^*_{s,i}}{\sqrt{\frac{4}{3}\alpha_{\mathrm{L},s} R^*_{s,i}}}\right]$$
$$R^*_{s,i}(t) = \sqrt{\frac{V^*_{s,i}(t)}{\pi n_s b_s}} \tag{3}$$
$$V^*_{s,i}(t) = \left[Q_{\mathrm{s,i}}(t_i - t_{i-1})\right] + V^*_{s,i-1}(t)$$

where t_i is the actual time, t_j is the time that the influent concentration was measured, and $\Delta C_{\mathrm{F}} = C_{\mathrm{F},j} - C_{\mathrm{F},j-1}$ and j denotes a measured influent concentration. For the first iteration ($j = 1$), $\Delta C_{\mathrm{F}} = C_{\mathrm{F},j} - C_{\mathrm{B}}$, where C_{B} is the background concentration measured prior to the start of recharge. At any time, t_i, the concentration at a monitoring well screen is determined through superposition given as:

$$C_{s,i}(r,t) = C_{\mathrm{B}} + \sum\nolimits_{j=1}^{j} C_{s,i,j}(r,t) \tag{4}$$

For a monitoring well with multiple screens, the total concentration could be calculated using a length- or flow-weighted average of $C_{s,i}(r,t)$ for the relevant screens.

Recharge flow rate of SWIFT water to the aquifer was quantified with a Rosemount 8750W Magnetic Flowmeter System immediately prior to entering TW-1. Because the recharge rate entering each screen (Q_i) is calculated based on a percentage of the total flow measured entering the recharge well, analysis was required to estimate (1) the flow distribution to each screen and (2) the variation in flow distribution over time. Sampling bias in wells with long screens is well documented in the literature (Reilly et al. 1989; Konikow and Hornberger 2006; Poulsen et al. 2019). This is a result of conventional monitoring wells lacking depth-discrete sampling mechanisms, an initial step was to evaluate the contribution of each screen to the observed breakthrough. Furthermore, low flow rates from the sampling pumps at the conventional wells (7.6 L/min) are likely to introduce bias in a well with multiple deep screens.

As sulfate was the most reliable of the six tracers (i.e., low influent variability, high number of samples, and had a clear breakthrough), it was used to determine where samples were collected at MW-UPA. First, a transport model for sulfate was calculated for each individual screen of TW-1 based on Eqs. (1)–(4). These models account for flow and transport in each strata of the UPA using the screen length (b), as determined from as-built diagrams and the original breakthrough work (Bullard et al. 2019), and aquifer characteristics (n and α) of each strata.

Depth- and flow-weighted average concentrations were calculated using the model-calculated breakthrough curves at monitoring well MW-UPA. Two separate flow-weighted averages were calculated, one based on prerehabilitation flow measured during initial conductivity breakthrough (Bullard et al. 2019), and the other based on postrehabilitation flow distribution measured during in-situ flowmeter testing in May 2019 (Martinez and Widdowson 2024). Details regarding pre- and postrehabilitation flow distribution are documented in Table 7. The length and flow weighted distributions were applied using all screens and using screens 1 and 2 only, based on observations that the upper screens were contributing more flow and mass. Using screens 1 and 2 proved to be the most effective in all cases; otherwise, a deterministic approach was employed to simulate tracer breakthrough. (see the ESM for further detail).

Results

Four distinct model scenarios were developed to simulate the tracer concentration data: (1) constant recharge concentrations and a constant rate of flow with time, as presented in Charbeneau (2000); (2) constant recharge concentrations with time, transient flow rate, and transient depth-variable flow distribution as derived by Bullard et al. (2019); (3) time-varying recharge concentrations, transient flow rate, and constant flow distribution; and (4) time-varying recharge concentrations, transient flow rate, and transient depth-variable flow distribution. Through comparison of the four mathematical models, sensitivity to recharge rate changes at the injection well and other operational conditions at the ALTR demonstration site were assessed.

The constant depth-variable flow distribution in scenario 3 is based on the initial conductivity breakthrough measured prior to the first rehabilitation of the recharge well (Bullard et al. 2019). For comparison, variable flow distribution was used in scenarios 2 and 4 based on the observation of a transient depth-variable flow distribution in TW-1. Three flow distributions are used, one based on the aforementioned prerehabilitation analysis and the other two based on postrehabilitation flow distributions measured using in-situ flowmeter testing. The flow distribution during phases 1–3 in scenarios 2 and 4 is equal to the initial prerehabilitation flow distribution. The flow distribution used in phase 6 was

Table 7 Pre- and postrehabilitation flow distributions and aquifer characteristics for MW-UPA

	Prerehabilitation flow distribution[a] (conductivity breakthrough)	Postrehabilitation flow distribution[b] (in situ flowmeter)	Porosity[a]	Longitudinal dispersivity[a] (ft [m])
Screen 1	18%	19%	0.20	5 [1.5]
Screen 2	24%	46%	0.25	10 [3.0]
Screen 3	6%	2%	0.27	10 [3.0]
Screen 4	9%	7%	0.35	20 [6.1]

[a]Bullard et al. 2019)

[b]Martinez and Widdowson (2024)

informed by flowmeter tests conducted at the end of phase 5 (Martinez and Widdowson 2024). The first flow distribution was based on additional flowmeter measurements conducted at the end of phase 8 following the second well rehabilitation (see the ESM for additional discussion of the process for determining the switch-back time).

Simulated breakthrough curves at well MW-UPA for each of the six intrinsic tracers are presented in Fig. 3. Starting with the conservative tracers (sulfate and chloride), scenario 1, while previously used at the SRC to describe initial breakthrough at MW-SAT, failed to capture observations on a larger spatial and time scale. This outcome was not unexpected based on transient recharge flow and concentration conditions at the SRC during the nine operational phases, and particularly the extended backflush (phase 2) and first interruption of recharge for well rehabilitation (phase 4). Overall, scenario 2 was effective in predicting initial breakthrough of conservative tracers, but because a constant influent concentration was assumed, the model results did not capture variations in sulfate and chloride concentrations following initial breakthrough at MW-UPA. Scenario 4 captured the breakthrough of sulfate but failed to accurately simulate chloride breakthrough for reasons described subsequently. In contrast to scenario 2, by accounting for the transient concentration of sulfate in SWIFT water, scenario 4 provided the best fit for postbreakthrough concentrations of sulfate. The accuracy of scenario 3 to capture the travel time of both conservative tracers was diminished by not accounting for the dynamic nature of flow distribution at TW-1 resulting from well rehabilitation.

Both scenarios 2 and 4 captured the peak breakthrough concentration of sulfate during the early time of phase 4 that followed the shutdown of operations (phase 3). However, scenario 2 accurately simulated the chloride breakthrough curve, whereas scenario 4 failed to capture time of travel or the chloride concentration breakthrough curve. This result may be due to the relatively large variability of chloride concentrations in SWIFT water with time compared to sulfate (Table 4) and particularly during the time period impacting breakthrough at MW-UPA (Fig. 2).

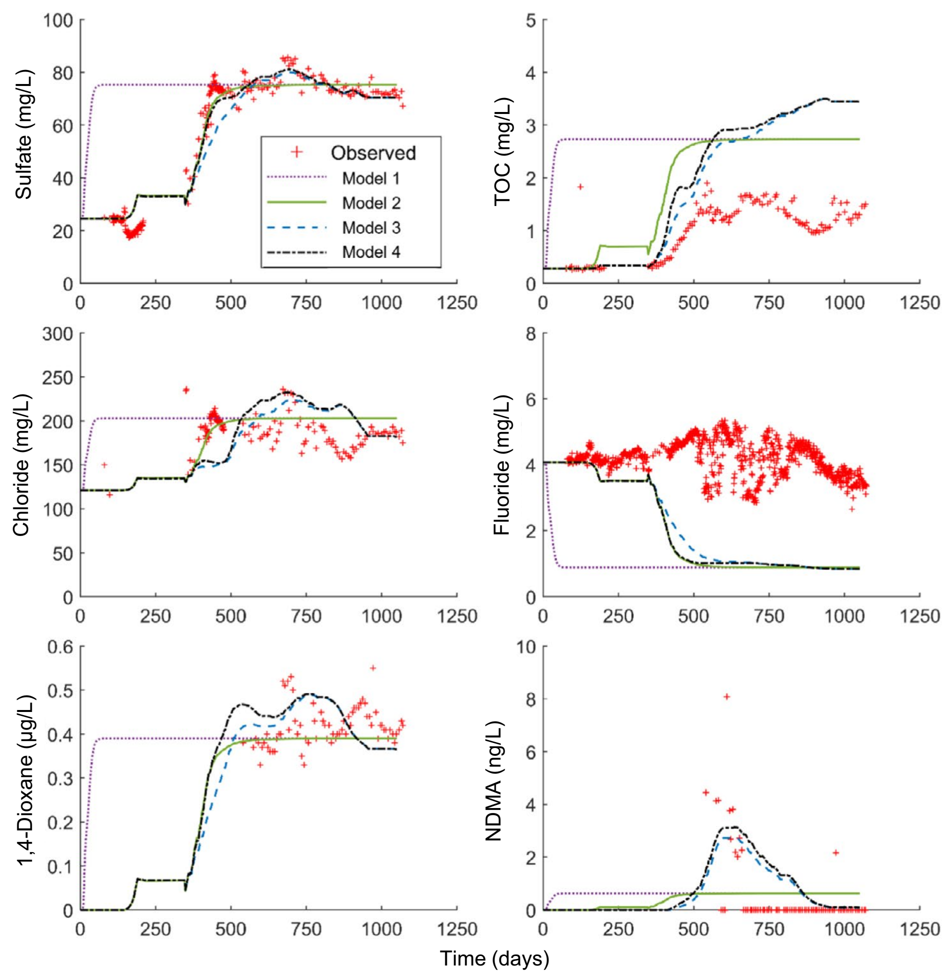

Fig. 3 Simulated and observed constituent concentrations at MW-UPA for the four model scenarios

These results reveal not only the sensitivity of time-variable recharge concentrations and recharge rates on simulation of breakthrough curves at the SRC, but also the discrepancy between sulfate and chloride as conservative tracers. However, the breakthrough time for both tracers was identical (400 days), which occurred during phase 5. The observed 400-day travel time at the SRC was significantly increased due to the 19-day period of pumping (phase 2) and the 159-day period of well maintenance without the recharge (phases 4 and 5) that preceded the breakthrough of sulfate and chloride during phase 6. By accounting for variable influent conditions and changing flow distribution following well rehabilitation, scenario 4 provided the best fit for sulfate. Coefficients of determination for all six tracers using scenario 4 are presented in Fig. 4.

Scenarios 3 and 4 simulated an earlier time of breakthrough for TOC and overpredicted the peak concentration following breakthrough (Fig. 3), whereas scenario 2 predicted a much earlier travel time and also failed to simulate the observed TOC breakthrough curve. As the models did not incorporate terms for attenuation, reactive mechanisms were not captured in the simulated TOC breakthrough concentration. In contrast with TOC and the conservative tracers (sulfate and chloride), fluoride concentrations in SWIFT water were below the background. As a result, the models predicted a lowering of fluoride concentrations with SWIFT water breakthrough. As shown in Fig. 3, fluoride concentrations in the UPA remained at background levels long after the observed breakthrough at MW-UPA, possibly indicating fluoride mobilization derived from the aquifer sediments.

Concentrations of 1,4-dioxane and NDMA were not measured until breakthrough was already identified, and therefore the initial breakthrough is not supported by observed measurements at the recharge well. Breakthrough of 1,4-dioxane is implied in the data given the time-averaged concentration in SWIFT water (0.39 µg/L). Scenarios 3 and 4 generally captured 1,4-dioxane concentrations following breakthrough. As shown in Fig. 2, NDMA was present intermittently in SWIFT water samples. Consistent with the simulation of 1,4-dioxane, by accounting for transient recharge concentrations, the peak concentrations of NDMA at MW-UPA were reflected in the scenario 3 and 4 simulations.

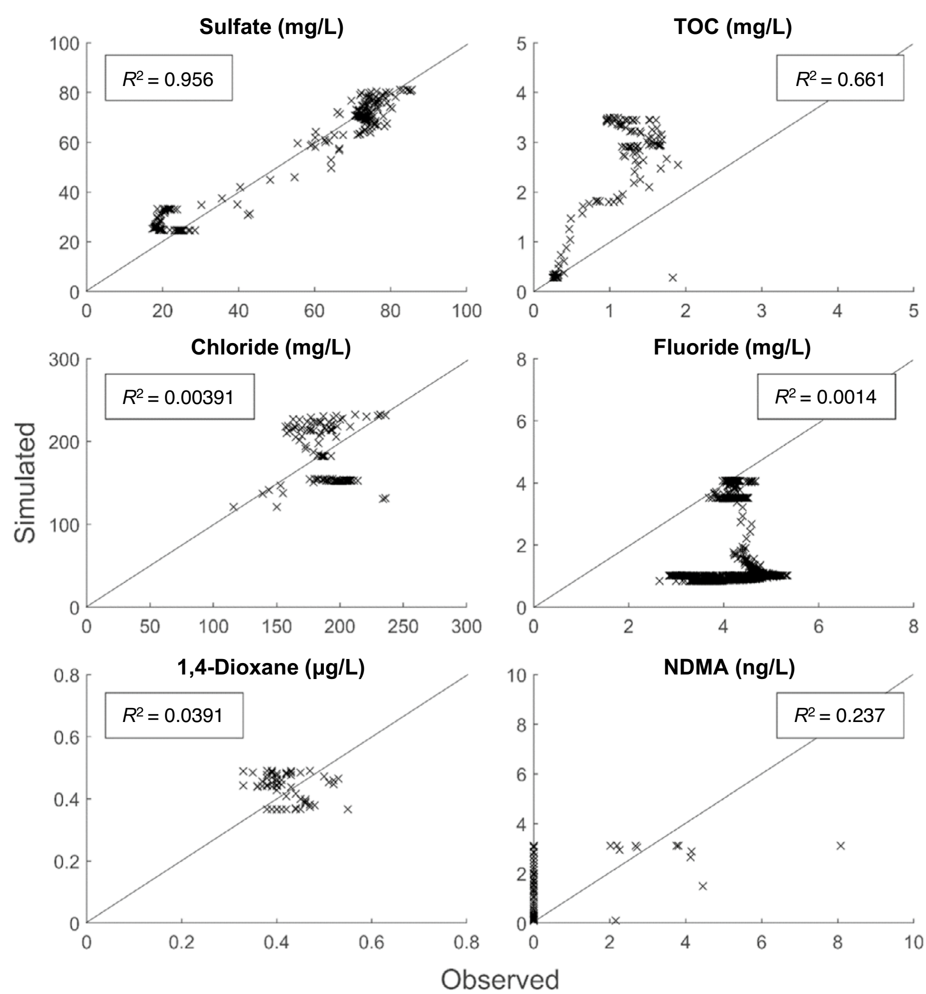

Fig. 4 Coefficient of determination for each constituent under model scenario 4

Discussion

The effectiveness of each of the potential tracers derived from SWIFT water varies along a spectrum, ranging from very effective to completely ineffective for characterizing solute transport and quantifying travel time to the UPA over a radial travel distance of 104 m. Each constituent will be discussed in the following subsections.

The radial transport model proved effective in simulating conservative tracer breakthrough at MW-UPA and provided insight into the tracer attenuation of other constituents. By accounting for transient boundary conditions (recharge concentration and flow rate), model scenario 4 served as the most effective analysis tool relative to the model scenarios based on sampling assumptions when representing recharge conditions over time (Fig. 3). Given the relatively long-term nature of the study and the variable operational conditions (Table 3), this finding may be a site specific. Breakthrough data at other MAR sites may be more effectively analyzed with simpler boundary conditions, depending on transport distances, recharge operations, and site hydrogeology.

Sulfate

Sulfate was the most effective conservative tracer for capturing breakthrough and travel time at the SRC. Multiple factors contributed to the efficacy of sulfate as a tracer in MW-UPA: (1) average sulfate concentrations in SWIFT water are significantly different (>3 SD) than native groundwater concentrations, which allowed for a clean breakthrough of SWIFT water sulfate concentrations; (2) with a few exceptions, influent sulfate concentrations had low variability with time and (3) high frequency of sulfate sampling allowed for more precise characterization of influent sulfate concentrations and therefore increased the accuracy of the model.

Chloride

Chloride was less reliable as a conservative tracer compared to sulfate but was still shown to be effective in confirming the sulfate travel time at MW-UPA. As noted previously, the significant range of chloride concentrations in SWIFT water as well as the relative similarity of native groundwater concentrations (within two standard deviations) compared to chloride in SWIFT water contributed to the reliability concerns. This variability lowered model effectiveness for tracking breakthrough and matching the trend in observed concentrations following breakthrough at MW-UPA.

Another line of evidence on the effectiveness of chloride as a tracer is the initial breakthrough observed at screen 1 of MW-SAT at the start of recharge operations (phase 1), in which chloride concentrations were higher than expected based on SWIFT water concentrations (Fig. 5). Before the start of recharge, the PAS in the immediate vicinity of TW-1 was conditioned with aluminum chlorohydrate (ACH) to stabilize the interstitial clays within the aquifer and maintain aquifer permeability once recharge began. Brown and Silvey (1977) reported that failure to pretreat the PAS will result in the loss of recharge well injectivity. It is possible that the higher chloride concentrations than expected in the initial breakthrough were a result of the remnants of this ACH treatment at TW-1 that was not fully recovered from screen 1.

As increased chloride concentrations were not observed in any other screens during the initial breakthrough at MW-SAT and limited to screen 1 (i.e., the UPA), and because native groundwater chloride concentrations are significantly higher in MW-MPA and MW-LPA, chloride is expected to be a more reliable tracer for the remaining conventional monitoring wells. In this case, chloride concentrations would be expected to decline with time as SWIFT water breakthrough is observed at these monitoring wells. Chloride concentration data from MW-MPA over the same period of performance showed indications of breakthrough of SWIFT water (Fig. 6). Application of the mathematical model to a different aquifer layer using scenario 4 confirmed a downward trend in chloride concentration over time, but without a sharp breakthrough (Fig. 6) (see ESM for further discussion).

TOC

Despite accounting for transient influent TOC concentrations, the mathematical model based on scenario 4 revealed limited success in simulating TOC breakthrough at the appropriate time and overpredicted observed breakthrough

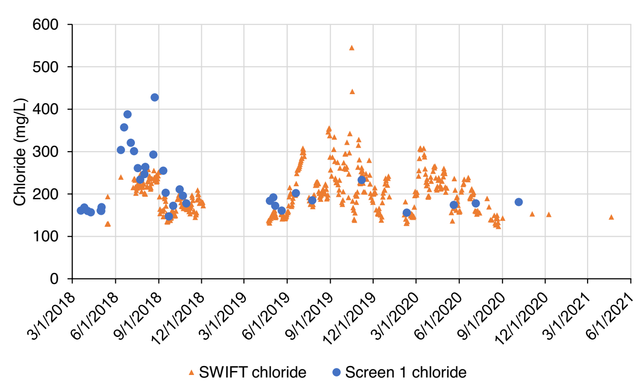

Fig. 5 Chloride concentrations in SWIFT water and MW-SAT screen 1. In the initial breakthrough period at MW-SAT (June 2018), observed concentrations at screen 1 were higher than influent SWIFT water concentrations. Delivery of SWIFT water to the PAS at chloride concentration > 200 mg/L was initiated on May 18, 2018

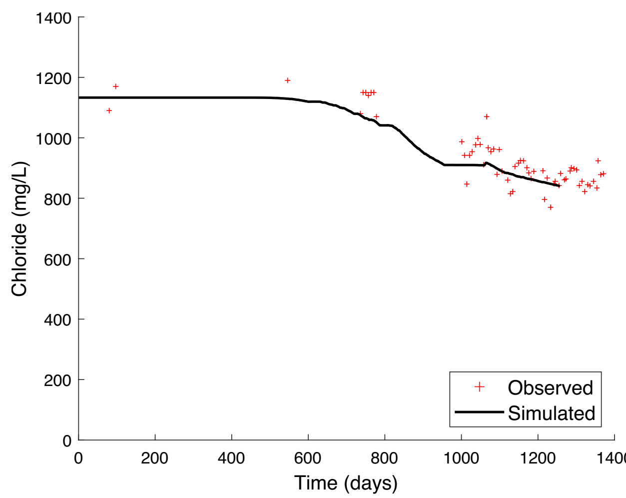

Fig. 6 Observed chloride concentration trend at MW-MPA over the period of performance compared to simulated breakthrough of SWIFT water based on model 4

concentrations. Departure from the conservative model was expected since TOC was shown to be a reactive SWIFT water constituent in a previous study, and the model did not account for the mass loss of the constituent during transport. The observed TOC concentrations reveal degradation with possibly limited sorption of the constituent within the aquifer system, which is common in direct injection conditions where the organic fraction of the soil is low (Patterson et al. 2011). With DO concentrations typically at or above saturation in SWIFT water (8–18 mg/L), aerobic biodegradation was a probable mechanism for the attenuation of TOC at the SRC. DO concentrations at MW-SAT indicate oxygen depletion and a return to suboxic to anoxic conditions present in the background PAS groundwater. Future work will aim to modify the approximation to include other attenuation mechanisms, including biodegradation, retardation, and abiotic reactions. Alternatively, a numerical model would provide greater capacity for capturing the complexities of transport coupled to attenuation compared to the approximation model presented here.

Fluoride

While fluoride was initially expected to be a reliable and conservative tracer, observed concentrations at MW-UPA showed no clear breakthrough signature compared to sulfate or chloride. This observation is consistent with previously observed fluoride concentrations in screen 1 during the initial breakthrough at MW-SAT (Bullard et al. 2019). Fluoride mobilization during MAR projects has been attributed to multiple causes, including mineral dissolution (Gaus et al. 2002; Schafer et al. 2018) and interaction with low permeability sediments within the aquifer system (Gaus et al. 2002; Malcuit et al. 2014). Schafer et al. (2018) hypothesized that fluoride release during MAR experiments was a result of the dissolution of carbonate-rich fluorapatite due to the injection of injectate with low ionic strength. In another ASR project, dual porosity mixing of recharge and native groundwater before recovery and slow dissolution of fluorite both contributed to elevated fluoride concentrations in recovered injectate (Gaus et al. 2002). Malcuit et al. (2014) observed fluoride concentrations from low permeability units contributing to elevated fluoride concentrations in a single-screened multilayer aquifer around the city of Bordeaux, France.

Elevated fluoride concentrations have been observed in the UPA of the Virginia Coastal Plain (Fig. S17 of the ESM) and in PAS groundwater in nearby Suffolk, Virginia (McFarland 2010). At the SRC, the highest fluoride concentrations are located at screens 1 and 2, from 152 to 215 m bgs, which is consistent with previous observations in the PAS. Since the UPA is a fluvial-deltaic sediment system, it lacks the fluorapatite and other phosphatic material common in marine systems, which are a common contributor to fluoride mobilization. McFarland (2010) hypothesizes that the high fluoride belt located in the UPA is a result of high-fluoride groundwater flowing from the overlying marine sediments into the PAS and adsorbing to oxyhydroxides within the PAS sediments. As sea level rises, the location of the saltwater transition zone shifts and causes fluoride to desorb due to adsorption of other anions in the saltwater zone, leading to elevated concentrations within the saltwater transition zone (McFarland 2010).

Though SWIFT water fluoride concentrations are low, fluoride continues to show elevated values at MW-UPA, even following observed breakthrough based on other constituents. This is hypothesized to be due to the continued desorption of fluoride from oxyhydroxides in the UPA due to increasing groundwater pH as SWIFT water is transported through the aquifer (LaFayette et al. 2020). As the mass of fluoride in the UPA does not increase with time, other than with the addition of SWIFT water, it is probable that once the fluoride in the native groundwater is desorbed, fluoride concentrations will decrease to SWIFT water levels. Therefore, fluoride is not a reliable tracer for this project but it may be a reliable tracer for other ALTR projects, depending on the local geochemistry and the difference between native groundwater fluoride and pH and the fluoride and pH of the AR.

1,4-dioxane and NDMA

A robust evaluation of the efficacy of 1,4-dioxane and NDMA as tracers was limited by the frequency of influent sampling as well as the number of detections. Due to their cost-effectiveness, sample frequency was lower for 1,4-dioxane and NDMA, and spikes or large variations in influent concentrations may not have been detected in the limited number of samples available. Furthermore, as only 16% of NDMA samples were above the 2 ng/L detection limit, it is probable that the remaining 84% of nondetects ranged from 0–2 ng/L and that tracer mass was not accounted for in the model. While previous research conducted at the SRC using columns packed with PAS sediment suggested that 1,4-dioxane and NDMA may degrade during transport (Dziura 2020), results from MW-UPA indicated that the two constituents are mostly conservative. This suggests that microbes that biodegrade these constituents may need a longer acclimation time with more consistent concentrations, and colonies large enough to degrade the constituents may not exist within the aquifer at the current time. Other studies have also indicated the need for a long acclimation period before degradation is observed (Drewes et al. 2006; Nalinakumari et al. 2010; Suzuki et al. 2015; Trussell et al. 2018). Sustained levels of peak 1,4-dioxane concentrations at MW-UPA indicate greater confidence in limited attenuation of 1,4-dioxane compared to NDMA.

Conclusions

During the period of performance at the SRC, three of the six intrinsic tracers examined served as indicators of conservative transport with varying degrees of confidence at the monitoring well (MW-UPA) located 104 m from the recharge well (TW-1). Given the variability of chloride concentrations in SWIFT water over time relative to sulfate, the results support the notion that sulfate was the most effective conservative tracer to describe travel time and conservative solute transport at the SRC. The third intrinsic tracer (1,4-dioxane) showed potential as a conservative tracer, but the analysis was limited by insufficient data during breakthrough at the observation well. However, consideration of 1,4-dioxane as an intrinsic tracer may be limited at many MAR projects due to state drinking-water standards and concern for health advisories.

An analytical model modified to account for variable operations at the MAR demonstration facility (scenario 4) was effective in simulating breakthrough curves at MW-UPA, particularly sulfate concentrations over the period of performance. This finding indicates the tracking of the front of recharge water at ALTR projects should incorporate time-varying recharge concentrations and transient flow rates. Furthermore, at sites with multiscreen injection wells, models should account for transient depth-variable flow distribution based on observed data or direct measurement.

The application of multiple intrinsic tracers to determine breakthrough in a multiaquifer system at the SRC demonstrates the significance of both a robust sampling plan and depth-discrete samples in a nearby multiscreen well for aquifer characterization. Comparing multiple tracers also aided in identifying tracer weaknesses and confirmed travel time to MW-UPA. For an intrinsic tracer, multiple factors contribute to the effectiveness of a constituent, including the difference between the tracer concentration in the recharge water and native groundwater, variability of tracer recharge concentrations, high frequency of influent sampling, and potential geochemical reactions.

The use of multiple tracers can confirm travel time with higher confidence, provide insight into attenuation and abiotic reactions, and guide monitoring decisions while scaling up ALTR projects. In a multiaquifer system like the PAS, tracer efficacy may vary by aquifer layer, and several background samples are beneficial to fully characterize the native groundwater before AR begins. Although the model developed and demonstrated in this study did not incorporate attenuation, a comparison of observed breakthrough data to model simulations provided semiquantitative evidence that attenuation impacted TOC transport and that fluoride was mobilized from aquifer sediment. In future ALTR projects, where the use of an artificial tracer can be cost-prohibitive, the further from the injection well being monitored, identification and monitoring of multiple, reliable intrinsic tracers will be an important part of ensuring the longevity of the project as well as understanding flow through large, complex aquifer systems.

Supplementary Information The online version contains supplementary material available at https://doi.org/10.1007/s10040-024-02846-3.

Acknowledgements The authors would like to thank members of the Hampton Roads Sanitation District (HRSD) SWIFT Research Center team and the HRSD CEL team for collection and analysis of samples.

Funding This work was supported by funding from the Hampton Roads Sanitation District (VT fund No. 466197) with M. Martinez partially supported by a Via Graduate Fellowship through the Charles E. Via, Jr. Department of Civil and Environmental Engineering at Virginia Tech.

Declarations

Conflicts of interest There are no conflicts of interest to declare.

References

Brown DL, Silvey WD (1977) Artificial recharge to a freshwater-sensitive brackish-water sand aquifer, Norfolk, Virginia. US Geol Surv Prof Pap 939. https://doi.org/10.3133/pp939

Bullard MG, Widdowson M, Salazar-Benites G, Heisig-Mitchell J, Nelson A, Bott C (2019) Managed aquifer recharge: transport and attenuation in a coastal plain aquifer. In: Proceedings of the EWRI World Environmental and Water Resources Congress 2019: Groundwater, Sustainability, Hydro-Climate/Climate Change, and Environmental Engineering. EWRI, Pittsburgh, PA, pp 1–14. https://doi.org/10.1061/9780784482346.011

Charbeneau RJ (2000) Groundwater hydraulics and pollutant transport. Prentice Hall, Upper Saddle River, NJ

Chen C-S (1985) Analytical and approximate solutions to radial dispersion from an injection well to a geological unit with simultaneous diffusion into adjacent strata. Water Resour Res 21(8):1069–1076. https://doi.org/10.1029/WR021i008p01069

Chen Y, Lu C, Luo J (2012) Solute transport in divergent radial flow with multistep pumping. Water Resour Res 48(2):1–10. https://doi.org/10.1029/2011WR010692

Davis SN, Campbell DJ, Bentley HW, Flynn TJ (1985) An introduction to ground-water tracers, EPA, Tuscon, AZ

Dillon P, Stuyfzand P, Grischek T, Lluria M, Pyne RDG, Jain RC, Bear J, et al (2019) Sixty years of global progress in managed aquifer recharge. Hydrogeol J 27:1–30. https://doi.org/10.1007/s10040-018-1841-z

Drewes JE, Hoppe C, Jennings T (2006) Fate and transport of N-nitrosamines under conditions simulating full-scale groundwater recharge operations. Water Environ Res 78(13):2466–2473. https://doi.org/10.2175/106143006X115408

Dziura T (2020) Evaluation of contaminant removal through soil aquifer treatment by a lab scale soil column experiment including a trace contaminant spike test. MSc Thesis, Virginia Tech, Blacksburg, VA

Gaus I, Shand P, Gale IN, Williams AT, Eastwood JC (2002) Geochemical modelling of fluoride concentration changes during Aquifer Storage and Recovery (ASR) in the Chalk aquifer in Wessex, England. Q J Eng Geol Hydrogeol 35(2):203–208. https://doi.org/10.1144/1470-9236/2001-52

Gerenday SP, Clark JF, Hansen J, Fischer I, Koreny J (2020) Sulfur hexafluoride and potassium bromide as groundwater tracers for managed aquifer recharge. Groundwater 58(5):777–787. https://doi.org/10.1111/gwat.12983

Goderniaux P, Brouyère S, Gutierrez A, Baran N (2010) Multi-tracer tests to evaluate the hydraulic setting of a complex aquifer system (Brévilles Spring Catchment, France). Hydrogeol J 18(7):1729–1740. https://doi.org/10.1007/s10040-010-0633-x

Goltz MN, Oxley ME (1991) Analytical modeling of aquifer decontamination by pumping when transport is affected by rate-limited sorption. Water Resour Res 27(4):547–556. https://doi.org/10.1029/90WR02760

Güven O, Falta RW, Molz FJ, Melville JG (1985) Analysis and interpretation of single-well tracer tests in stratified aquifers. Water Resour Res 21(5):676–684. https://doi.org/10.1029/WR021i005p00676

Hadi K, Saravana Kumar U, Al-Senafy M, Mukhopadhyay A, Al-Khalid A, Al-Fahad K, Bhandary H (2016) Multi-well and multi-tracer tests to characterize the groundwater aquifers in southern Kuwait. Environ Earth Sci 75(20):1340. https://doi.org/10.1007/s12665-016-6143-y

Heywood CE, Pope JP (2009) Simulation of groundwater flow in the coastal plain aquifer system of Virginia. US Geol Surv Sci Invest Rep 2009-5039. https://doi.org/10.3133/sir20095039

Hillebrand O, Nödler K, Sauter M, Licha T (2015) Multitracer experiment to evaluate the attenuation of selected organic micropollutants in a karst aquifer. Sci Total Environ 506–507(February):338–343. https://doi.org/10.1016/j.scitotenv.2014.10.102

Hsieh PA (1986) A new formula for the analytical solution of the radial dispersion problem. Water Resour Res 22(11):1597–1605. https://doi.org/10.1029/WR022i011p01597

Hunt B (1986) Solutions for steady groundwater flow in multi-layer aquifer systems. Trans Porous Media 1:419–429

Konikow LF, Hornberger GZ (2006) Modeling effects of multinode wells on solute transport. Ground Water 44(5):648–660. https://doi.org/10.1111/j.1745-6584.2006.00231.x

LaFayette GN, Knappett PSK, Li Y, Loza-Aguirre I, Polizzotto ML (2020) Geogenic sources and chemical controls on fluoride release to groundwater in the independence basin, Mexico. Appl Geochem 123:104787. https://doi.org/10.1016/j.apgeochem.2020.104787

Lai K-H, Liu C-W, Liang C-P, Chen J-S, Sie B-R (2016) A novel method for analytically solving a radial advection-dispersion equation. J Hydrol 542(November):532–540. https://doi.org/10.1016/j.jhydrol.2016.09.027

Lipps WC, Braun-Howland EB, Baxter TE (eds) (2023) Standard methods for the examination of water and wastewater, 24th edn. APHA Press, Washington, DC

Malcuit E, Atteia O, Larroque F, Franceschi M, Pryet A (2014) On the role of low-permeability beds in the acquisition of F and SO4 concentrations in a multi-layer aquifer, South-West France. J Contam Hydrol 169:37–49. https://doi.org/10.1016/j.jconhyd.2014.05.001

Martinez MB, Widdowson MA (2024) Evaluating flow distribution in a multiaquifer recharge well using an in situ flowmeter. Groundwater. https://doi.org/10.1111/gwat.13379

Martinez MB, Widdowson MA, Bott C, Holloway D, Heisig-Mitchell J, Wilson C (2022) Demonstration of managed aquifer recharge in a coastal plain aquifer: lessons learned. Groundwater. https://doi.org/10.1111/gwat.13197

McFarland ER (2010) Groundwater-quality data and regional trends in the Virginia Coastal Plain, 1906–2007. US Geol Surv Prof Pap 1772. https://pubs.usgs.gov/pp/1772/. Accessed Oct 2021

McFarland ER (2013) Sediment distribution and hydrologic conditions of the Potomac aquifer in Virginia and parts of Maryland and North Carolina. US Geol Surv Sci Invest Rep 2013–5116, 67 pp. http://pubs.usgs.gov/sir/2013/5116/

McFarland ER, Bruce TS (2006) The Virginia coastal plain hydrogeologic framework. US Geol Surv Prof Pap 1731, 118 pp

Meng AA, III, Harsh JF (1988) Hydrogeologic framework of the Virginia Coastal Plain. US Geol Surv Prof Pap 1404-C, 82 pp

Mirecki JE, Campbell BG, Conlon KJ, Petkewich MD (1998) Solute changes during aquifer storage recovery testing in a limestone/clastic aquifer. Ground Water 36(3):394–403. https://doi.org/10.1111/j.1745-6584.1998.tb02809.x

Moench AF (1989) Convergent radial dispersion: a Laplace transform solution for aquifer tracer testing. Water Resour Res 25(3):439–447. https://doi.org/10.1029/WR025i003p00439

Moench AF (1995) Convergent radial dispersion in a double-porosity aquifer with fracture skin: analytical solution and application to a field experiment in fractured chalk. Water Resour Res 31(8):1823–1835. https://doi.org/10.1029/95WR01275

Molz FJ, Melville JG, Güven O, Crocker RD, Matteson KT (1985) Design and performance of single-well tracer tests at the mobile site. Water Resour Res 21(10):1497–1502. https://doi.org/10.1029/WR021i010p01497

Molz FJ, Güven O, Melville JG, Crocker RD, Matteson KT (1986) Performance, analysis, and simulation of a two-well tracer test at the mobile site. Water Resour Res 22(7):1031–1037. https://doi.org/10.1029/WR022i007p01031

Molz FJ, Güven O, Melville JG, Nohrstedt JS, Overholtzer JK (1988) Forced-gradient tracer tests and inferred hydraulic conductivity distributions at the mobile site. Ground Water 26(5):570–579. https://doi.org/10.1111/j.1745-6584.1988.tb00790.x

Munch JW (2005) Method 521: determination of nitrosamines in drinking water by solid phase extraction and capillary column gas chromatography with large volume injection and chemical ionization tandem mass spectrometry (MS/MS). US Environmental Protection Agency, Washington, DC

Munch JW, Grimmett P (2008) Method 522: determination of 1,4-dioxane in drinking water by solid phase extraction (SPE) and gas chromatography mass spectrometry (GC/MS) with selected ion monitoring (SIM). US Environmental Protection Agency, Washington, DC

Nalinakumari B, Cha W, Fox P (2010) Effects of primary substrate concentration on NDMA transport during simulated aquifer recharge. J Environ Eng 136(4):363–370. https://doi.org/10.1061/(ASCE)EE.1943-7870.0000168

Novakowski KS (1992) The analysis of tracer experiments conducted in divergent radial flow fields. Water Resour Res 28(12):3215–3225. https://doi.org/10.1029/92WR01722

Patterson BM, Shackleton M, Furness AJ, Bekele E, Pearce J, Linge KL, Busetti F, Spadek T, Toze S (2011) Behaviour and fate of nine recycled water trace organics during managed aquifer recharge in an aerobic aquifer. J Contam Hydrol 122(1–4):53–62. https://doi.org/10.1016/j.jconhyd.2010.11.003

Pavelic P, Dillon PJ, Simmons CT (2006) Multiscale characterization of a heterogeneous aquifer using an ASR operation. Ground Water 44(2):155–164. https://doi.org/10.1111/j.1745-6584.2005.00135.x

Pfaff JD (1993) Method 300.0 determination of inorganic anions by ion chromatography. US Environmental Protection Agency, Cincinnati, OH

Poulsen DL, Cook PG, Simmons CT, McCallum JL, Dogramaci S (2019) Effects of intraborehole flow on purging and sampling long-screened or open wells. Groundwater 57(2):269–278. https://doi.org/10.1111/gwat.12797

Pyne RDG (2006) Groundwater recharge and wells: a guide to aquifer storage recovery, 2nd edn. CRC, San Diego

Reilly ET, Franke OL, Bennett GD (1989) Bias in groundwater samples caused by wellbore flow. J Hydraul Eng 115(2):270–276. https://doi.org/10.1061/(ASCE)0733-9429(1989)115:2(270)

Reimus P, Pohll G, Mihevc T, Chapman J, Haga M, Lyles B, Kosinski S, Niswonger R, Sanders P (2003) Testing and parameterizing a conceptual model for solute transport in a fractured granite using multiple tracers in a forced-gradient test. Water Resour Res 39(12). https://doi.org/10.1029/2002WR001597

Ringleb J, Sallwey J, Stefan C (2016) Assessment of managed aquifer recharge through modeling: a review. Water (Switzerland) 8(12):1–32. https://doi.org/10.3390/w8120579

Sanford WE, Plummer LN, Casile G, Busenberg E, Nelms DL, Schlosser P (2017) Using dual-domain advective-transport simulation to reconcile multiple-tracer ages and estimate dual-porosity transport parameters. Water Resour Res 53(6):5002–5016. https://doi.org/10.1002/2016WR019469

Schafer D, Donn M, Atteia O, Sun J, MacRae C, Raven M, Pejcic B, Prommer H (2018) Fluoride and phosphate release from carbonate-rich fluorapatite during managed aquifer recharge. J Hydrol 562(July):809–820. https://doi.org/10.1016/j.jhydrol.2018.05.043

Suckow A, Deslandes A, Raiber M, Taylor AR, Davies P, Gerber C, Leaney F (2020) Reconciling contradictory environmental tracer ages in multi-tracer studies to characterize the aquifer and quantify deep groundwater flow: an example from the Hutton Sandstone, Great Artesian Basin, Australia. Hydrogeol J 28:75–87. https://doi.org/10.1007/s10040-019-02042-8

Suzuki R, Kameda I, Takabe Y, Nishimura F, Itoh S (2015) Removal of dissolved organic matter and disinfection by-products formation potential in the upper layer during soil aquifer treatment. J Water Environ Technol 13(2):107–118. https://doi.org/10.2965/jwet.2015.107

Székely F (1992) Pumping test data analysis in wells with multiple or long screens. J Hydrol 132:137–156. https://doi.org/10.1016/0022-1694(92)90176-V

Trussell B, Trussell S, Qu Y, Gerringer F, Stanczak S, Venezia T, Monroy I, Bacaro F, Trussell R (2018) A four-year simulation of soil aquifer treatment using columns filled with San Gabriel Valley sand. Water Res 144(November):26–35. https://doi.org/10.1016/j.watres.2018.07.012

West LJ, Odling NE (2007) Characterization of a multilayer aquifer using open well dilution tests. Ground Water 45(1):74–84. https://doi.org/10.1111/j.1745-6584.2006.00262.x

Williams AT (2000) Using an aquifer storage and recovery (ASR) trial as a large scale tracer test. In: Dassargues A (ed) Tracers and modelling in hydrogeology. IAHS, Liege, Belgium, pp 195–199

Wu Y-X, Wu H-N, Shen S-L, Xu Y-S (2015) Behaviour of multi-aquifer system during pumping test. Jpn Geotech Soc Spec Publ 1(4):15–18. https://doi.org/10.3208/jgssp.CPN-11

Young SC, Benton DJ (1990) The usefulness of multi-well aquifer tests in heterogeneous aquifers. AECL report, Atomic Energy of Canada, Chalk River, ON